Supporting Information

Liu et al. 10.1073/pnas.1213235110

SI Materials and Methods

Plant Materials and Growth Conditions. All *Arabidopsis thaliana* L. (Heynh) lines used in the study are in the Columbia (Col-0) background. The *amp1-1* line was obtained from the *Arabidopsis* Biological Resource Center. The *nox1* mutant was described in our previous study (1). Plants were grown on soil (Scotts Metro-Mix 200), or on petri dishes (100 × 15 mm) containing half-strength MS media (Gibco), 1% (wt/vol) sucrose (Sigma), and 0.8% (wt/vol) agar (Becton Dickinson) in controlled environmental rooms at ∼22 °C and at a photon fluency rate of ∼100 $\mu mol \cdot m^{-2} \cdot s^{-1}$. Photoperiods were 16-h light/8-h dark cycles. *Trans*-zeatin (Sigma), at the concentrations indicated, was added directly to the MS media. Sodium nitroprusside (SNP; Sigma), at the concentrations indicated, was placed with agar just on the inner side of petri dish's cover to avoid the direct contact of SNP chemical with *Arabidopsis* seedlings, ensuring that the plants were specifically exposed to gaseous NO.

Isolation of Continuous NO-Unstressed Mutants. For the genetic screen, T-DNA insertion-mutagenized *Arabidopsis* (Col-0) seeds were obtained from the Arabidopsis Biological Resource Center and Ethyl methane sulfonate (EMS)-mutagenized seeds were either obtained from Lehle Seeds or generated according to a standard procedure. These seeds were plated on growth medium containing 120 μM SNP for 10 d. Seedlings with large green leaves were selected as putative mutants and transplanted to SNP-free medium for 7 d and then to soil to obtain seeds. Putative mutants were rescreened for two more generations, and any line retaining the phenotype was designated as *continuous NO-unstressed* (*cnu*). The *cnu1-1* and *cnu1-2* mutants were isolated from T-DNA insertion pools and EMS pools, respectively, and identified to be allelic through genetic analysis.

Analysis of Flowering Time. It has been shown that flowering time is closely related to the number of leaves produced on the primary stem before the first flower is initiated, and late-flowering plants form more leaves. For soil-grown plants, we scored the number of rosette leaves and days to flowering at the stage when the first flower was appearing, as performed previously (1). Because *cnu1* and *amp1* produces more leaves before flowering, which is not related to flowering time, we analyzed flowering time by days to flowering. For seedlings grown on petri dishes, because it was difficult to score the number of leaves at the stage of flowering, we scored the number of rosette leaves at the stage of bolting when stems were about 3 mm and the number of days to bolting, both as described previously (1).

Analysis of *FLOWERING LOCUS C* and *FLOWERING TIME* mRNA Abundance. The abundance of mRNAs was analyzed as described previously (1). Seedlings were grown on soil or petri dishes for 10–12 d under 16-h light/8-h dark cycles. Shoots from 10 seedlings were collected 8 h after dawn for analyzing single-time-point mRNA abundance. Total mRNAs were prepared and reverse transcribed using a cDNA synthesis kit (Invitrogen). Primers used for the PCR reactions were as follows: *FLOWERING TIME* (*FT*), 5′-actatataggcatcatcaccgttcgttactcg, 5′-acaactg-gaacaacctttggcaatg (2); *Ubiquitin10* (*UBQ*), 5′-taaaaactttctcaat-tctctct, 5′-ttgtcgatggtgtcggagctt. For PCR reactions, 25 cycles were used for *FT* and 20 cycles for *UBQ*, which are small numbers of cycles to ensure detection in the linear part of the amplification range. PCR products were detected by standard Southern blot using radioactively ^{32}P-labeled probes. *FLOWERING LOCUS C* (*FLC*) mRNA abundance was detected using standard Northern blot as described (1), using probes made from the *FLC* clone, which were kind gifts from R. Amasino (University of Wisconsin, Madison, WI). Total RNA (10 μg) was separated, transferred to a hybridization transfer membrane (PerkinElmer), and blotted with respective ^{32}P-labeled probes. The levels of mRNAs were normalized against the signal obtained by hybridizing the same blot or the same RT-PCR samples with an *UBQ* probe. The abundance of mRNAs was further quantified using Image J (http://rsb.info.nih.gov/ij/), as described previously (1).

Positional Identification of *cnu1-1*. We backcrossed *cnu1-1* to WT (Col-0) three times. The homozygous *cnu1-1* line in the Col-0 background was crossed to the polymorphic ecotype L*er* and followed by self-pollinating F_1 progeny to yield an F_2 mapping population of 1,800 chromosomes. Linkage analysis of F_2 plants revealed that the *cnu1* locus locates in chromosome 3. Fine mapping markers were chosen using http://Arabidopsis.org, MapViewer Home. These markers were used to perform PCR and isolated the interval that flanks the mutation. The *CNU1-1* mutation was further identified by PCR analysis of gene-coding regions and confirmed by sequencing the *ALTERED MERISTEM PROGRAM1* (AMP1) coding region. The *CNU1-2* mutation was identified by sequencing the AMP1 coding region.

Analysis of NO Levels. Endogenous NO levels were analyzed using an NO-sensitive dye, 4,5-diaminofluorescein diacetate (DAF-2DA) (3), as performed previously (1). For DAF-2DA imaging, *Arabidopsis* seedlings were grown on soil under long days. Rosette leaves were collected 8 h after dawn, incubated in a solution containing 0.1 mM $CaCl_2$, 10 mM KCl, and 10 mM Mes-Tris, pH 5.6, for 2 h, and stained with 10 μM DAF-2DA (Molecular Probes) for 45 min. These leaves were analyzed using a fluorescence stereomicroscope (Stemi SV 11; Zeiss) equipped with a CCD camera. The excitation was provided at 495 nm, and the emission images at 515 nm were obtained with a constant acquisition time. The images were further processed and analyzed using Image J (http://rsb.info.nih.gov/ij/).

Chemicals Used for Analyzing the Reaction of Zeatin and Peroxynitrite. *Trans*-zeatin, sodium nitrite, and H_2O_2 (30%, wt/wt) were obtained from Sigma. NMR solvents and DMSO-d_6 were obtained from Cambridge Isotope Laboratories. All solvents were HPLC grade. All other chemicals were the highest analytical grade available from Sigma. Deionized water (≥18 MΩ/cm) was used in the preparation of buffers and reagents. Hydrogen peroxide in stock solutions was measured based on the absorbance at 240 nm (ε = 41 $L \cdot M^{-1} \cdot cm^{-1}$).

Reaction of *Trans*-zeatin with Peroxynitrite In Vitro. Peroxynitrite was synthesized using two methods as described previously: sodium nitrite and hydrogen peroxide (H_2O_2) (4) and isoamyl nitrite and H_2O_2 (5). The concentration of peroxynitrite was determined by measuring its UV absorbance at 302 nm ($\varepsilon_{302\ nm}$ = 1,670 $L \cdot M^{-1} \cdot cm^{-1}$) as described (4, 5). The synthesized peroxynitrite was store at −20 °C and used within a week. *Trans*-zeatin (0.2 mM) was incubated with peroxynitrite (0.2 mM) under constant stirring in 100 mM sodium phosphate buffer (pH range from 4.3 to 10.5, preferably at pH 9.5) containing 0.1 mM diethylenetriaminepentaacetic acid (DTPA) for 5 min at 37 °C. An appropriate amount of HCl was then used to neutralize NaOH in the peroxynitrite solution. The products were determined by either HPLC (ZORBAX Eclipse Plus C_{18} column, 2.1 × 150

mm, 5 μm; ZORBAX SB-C_8 guard column, 4.6 × 15 mm, 5 μm) using 0.25% acetic acid in acetonitrile water (25:75, vol/vol) with a photodiode-array detector, or HPLC-MS/MS, performed using a Finnigan LCQ (ThermoFinnigan).

Purification of Products Formed by the Reaction of *Trans*-zeatin and Peroxynitrite. Under constant stirring, peroxynitrite was added at a final concentration of 2 mM to a reaction buffer containing 2 mM *trans*-zeatin, 0.1 mM DTPA, and 100 mM sodium phosphate buffer (pH range from 4.3 to 10.5, preferably at pH 9.5) for 5 min at 37 °C, as described above. The reaction buffer was adjusted to pH = 8.0 and loaded onto C_{18} cartridges (1 g, 6 mL; Agilent) for desalting and concentrating. The C_{18} cartridges were first washed with water (pH = 8.0) and then eluted with methanol. The solution was concentrated and separated by semi-HPLC (Delta 600; Waters), and 0.5 mL of the reaction mixture was injected directly onto a preparative reverse-phase column (ZORBAX Eclipse XDB-C_{18}, 9.4 × 250 mm, 7 μm with a guard column; ZORBAX SB-C_8, 9.4 × 15 mm, 7 μm; Agilent). Separations were carried out under isocratic conditions with 0.25% acetic acid in acetonitrile-water (25:75, vol/vol) at a flow rate of 3.0 mL/min and monitored by a UV spectrophotometer at 300 nm. The reaction and purification were repeated several times to obtain enough material for further analyses.

Characterization of the Reaction Products. UV-visible spectra were obtained at various pH values using a TU-1901 Diode Array Spectrophotometer (Beijing Purkinje General Instrument). HPLC analyses were performed using a pump equipped with a Surveyor Diode Array Detector (ThermoFinnigan). LC-MS analyses were carried out using a ZORBAX Eclipse Plus C_{18} column (2.1 × 150 mm, 5 μm) under isocratic conditions with 0.25% acetic acid in acetonitrile water (25:75, vol/vol) at a flow rate of 0.25 mL/min. The electrospray mass spectra and MS/MS spectra were recorded on an ion trap mass spectrometer (LCQ Advantage; ThermoFinnigan) equipped with an electrospray ionization source. The analytical conditions were 220 °C capillary temperature, 4.5-kV source voltage, 10-V capillary voltage, and 15-V tube lens offset. The collision energy (CE) was changed from 20 to 30 to obtain a better resolution. High-resolution (HR) electrospray ionization (ESI) mass spectra were obtained on a JMS-700 (JEOL) in a positive ion mode in a spraying solution containing 0.25% acetic acid in acetonitrile water (25:75, vol/vol). ^{1}H, and ^{13}C NMR, ^{1}H–^{1}H Correlation Spectroscopy (COSY), and ^{1}H–^{13}C Heteronuclear Multiple Quantum Correlation (HMQC) spectra were recorded on a Bruker DRX 400-MHz instrument in DMSO-d_6 using standard pulse programs. ^{1}H and ^{13}C chemical shifts were referenced to the internal solvent DMSO-d_6. Chemical reduction of the isolated compounds was carried out under two different conditions: (*i*) excess sodium hydrosulfite in 100 mM Tris-HCl and (*ii*) metallic iron powder in 12 M HCl (4, 6).

Characterization of Product A Purified from Plant Tissues. Ten grams of fresh plant material was homogenized in liquid nitrogen and incubated in 10 mL of cold (−20 °C) extraction mixture consisting of methanol, water, and formic acid (15:4:1, vol/vol/vol). After overnight extraction at −20 °C, solids were separated by centrifugation (20,000 × *g*, 15 min) and reextracted for 30 min in an additional 5 mL of the extraction mixture at −20 °C. The supernatants were pooled and passed through a Sep-Pak Plus C_{18} cartridge to remove lipids and some plant pigments and evaporated until the methanol was completely removed. The residue was redissolved in 5 mL of 1 M formic acid and applied to an Oasis MCX column preconditioned with 5 mL of methanol followed by 5 mL of 1 M formic acid. The column was washed with 5 mL of 1 M formic acid, methanol, and 0.35 M ammonium hydroxide and then eluted with 5 mL of 0.35 M ammonium hydroxide in methanol. This process was repeated five times, and all of the eluted solution was combined, evaporated at 40 °C under N_2, and then redissolved in 0.5 mL of methanol, water, and formic acid (15:4:1, vol/vol/vol).

Samples were dissolved in the mobile phase, filtered through a microfilter [Polytetrafluoroethylene (PTFE), 0.45 μM; Waters], and 20 μL of the sample solution was injected into a reverse-phase (RP) column (ZORBAX Eclipse Plus C_{18} column, 2.1 × 150 mm, 5 μm; ZORBAX SB-C_8, 4.6 × 15 mm, 5 μm; a guard column). The column temperature was set at 30 °C. Solvent A consisted of 0.25% acetic acid and solvent B consisted of acetonitrile. At a flow rate of 0.25 mL/min, the following binary gradient was used: 0–3 min, 82% solvent A and 3.1–12.0 min, 75% solvent A, followed by 5 min of isocratic elution with 50% solvent A, and finally equilibration to initial conditions for 10 min.

For the ion trap mass spectrometer (LCQ Advantage; ThermoFinnigan), equipped with an electrospray ionization source, the following conditions were used: capillary temperature, 220 °C; source voltage, 4.5 kV; capillary voltage, 10 V; tube lens offset, 15 V. The CE was changed from 20 to 30 to obtain better resolution. Qualitative analysis was done by HPLC-MS and HPLC-MS/MS, and the spectra were compared with the standards (8-nitro-zeatin, N^6-nitro-zeatin, and N^6-nitroso-zeatin) obtained from reaction products in vitro.

1. He Y, et al. (2004) Nitric oxide represses the Arabidopsis floral transition. *Science* 305 (5692):1968–1971.
2. Cerdán PD, Chory J (2003) Regulation of flowering time by light quality. *Nature* 423 (6942):881–885.
3. Lamattina L, García-Mata C, Graziano M, Pagnussat G (2003) Nitric oxide: The versatility of an extensive signal molecule. *Annu Rev Plant Biol* 54:109–136.
4. Yermilov V, et al. (1995) Formation of 8-nitroguanine by the reaction of guanine with peroxynitrite in vitro. *Carcinogenesis* 16(9):2045–2050.
5. Uppu RM (2006) Synthesis of peroxynitrite using isoamyl nitrite and hydrogen peroxide in a homogeneous solvent system. *Anal Biochem* 354(2):165–168.
6. Douki T, Cadet J, Ames BN (1996) An adduct between peroxynitrite and 2′-deoxyguanosine: 4,5-dihydro-5-hydroxy-4-(nitrosooxy)-2′-deoxyguanosine. *Chem Res Toxicol* 9(1):3–7.

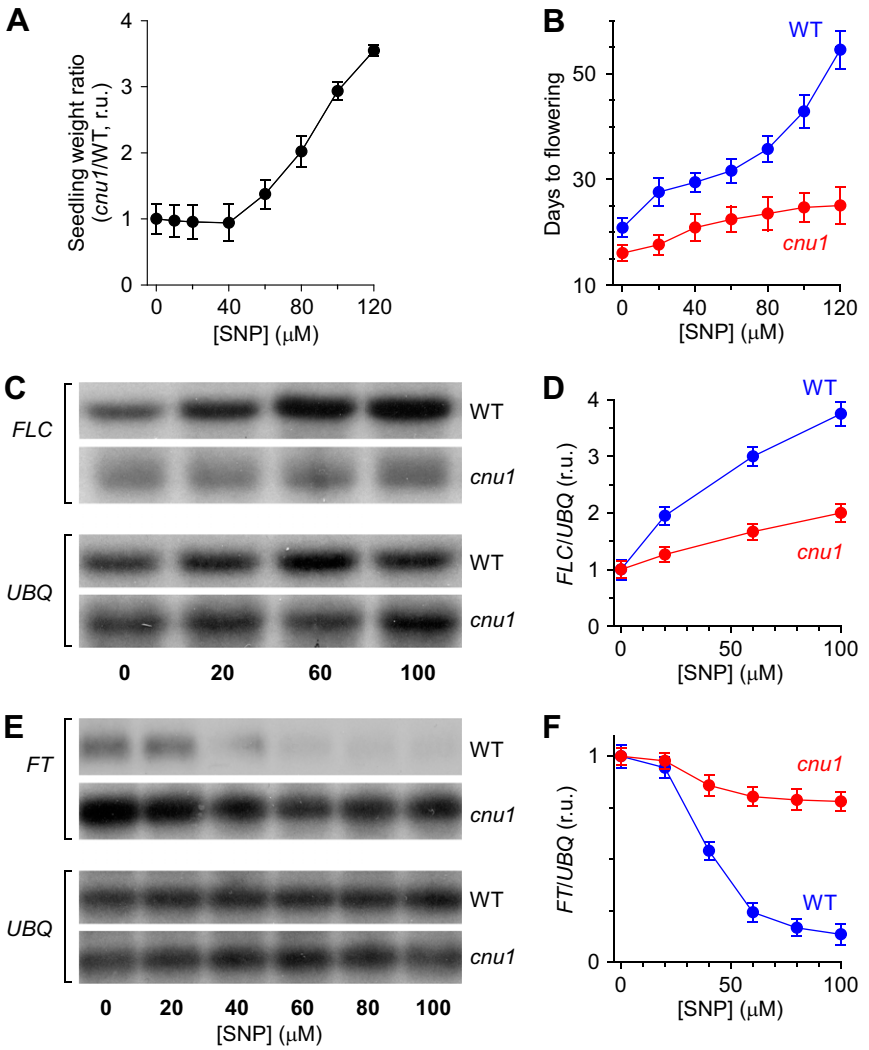

Fig. S1. The *cnu1* phenotype of seedling growth and flowering time insensitive to SNP. (*A*) Comparative analysis of the *cnu1* seedling growth in response to SNP. WT and *cnu1* seedlings were grown on MS media containing several concentrations of SNP for 3 wk as described in Fig. 1 *A* and *B*. The ratio between *cnu1* seedling weight and WT seedling weight was plotted as a function of applied concentrations of SNP, an NO donor (mean ± SD; $n = 150$ seedlings). The ratio at 0 μM SNP was arbitrarily set to 1 (r.u., relative unit). (*B*) Quantitative analysis of flowering time for the *cnu1* and WT grown on petri dishes under 16-h light/8-h dark regime and at the concentrations of SNP ranging from 0 to 120 μM. Data from six separate experiments are shown (mean ± SD; $n = 120$ plants). (*C* and *E*) The mRNA abundance of *FLC* (*C*) and *FT* (*E*) in *cnu1* and WT in response to SNP treatment. Plants were grown on the media containing several concentrations of SNP for 9 d as described in *B*, and shoots were harvested 8 h after dawn. *FLC* and *FT* mRNA abundance was analyzed using Northern blot and RT-PCR, respectively. *UBQ* mRNA was used as a loading control. Similar results were seen in three independent experiments. (*D* and *F*) Quantitative analysis of the mRNA abundance of *FLC* (*D*) and *FT* (*F*) from experiments as in *C* and *E*, respectively. The mRNA levels were normalized to *UBQ* mRNA levels with the value at 0 μM SNP set arbitrarily to 1 (r.u., relative unit).

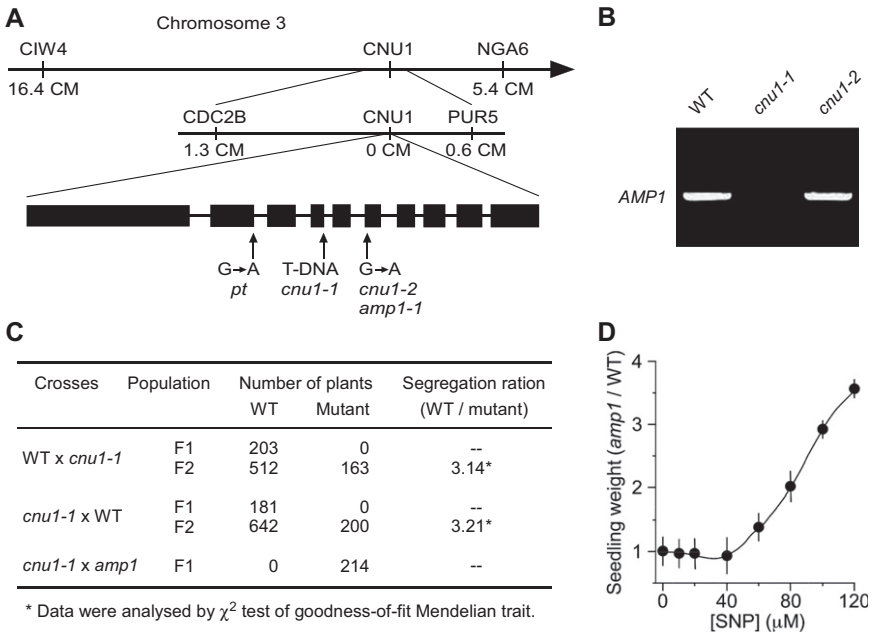

Crosses	Population	Number of plants WT	Number of plants Mutant	Segregation ration (WT / mutant)
WT x *cnu1-1*	F1	203	0	--
	F2	512	163	3.14*
cnu1-1 x WT	F1	181	0	--
	F2	642	200	3.21*
cnu1-1 x *amp1*	F1	0	214	--

* Data were analysed by χ^2 test of goodness-of-fit Mendelian trait.

Fig. S2. Map-based cloning reveals that *CNU1* is identical to *AMP1*. (*A*) *CNU1* was mapped to a region of chromosome 3 by analyzing 1,800 recombinant chromosomes from F_2 seedlings derived from a *cnu1* × L*er* cross with molecular markers. Sequencing analysis of AMP1 genomic region in *cnu1* mutants identified the T-DNA insertion in the end of fourth exon in *cnu1-1* and a G to A point mutation in *cnu1-2*, which is identical the mutation in *amp1-1*. (*B*) PCR analysis shows that *AMP1* was amplified in *cnu1-2* that carries a point mutation and WT but not in *cnu1-1* due to a T-DNA insertion. The primers for *AMP1* analyses were 5′-ttcgtcgccactttctacactctc and 5′-ttattccctctgatgcgttcatcg. (*C*) Genetic analysis shows that *cnu1-1* and *cnu1-2* are allelic to *amp1*. All F1 seedlings derived from WT × *cnu1* and *cnu1* × WT crosses showed seedling growth insensitive to 120 μM SNP. F_2 seedlings showed a 3:1 WT:*cnu1-1* segregation, suggesting that *cnu1-1* carries a recessive mutation. All F_1 seedlings derived from a *cnu1* × *amp1-1* cross showed a *cnu1* phenotype in seedling growth, suggesting that *cnu1* is allelic to *amp1*. (*D*) The *amp1-1* mutant displayed seedling growth insensitivity to SNP similar to *cnu1* mutants. The experimental conditions and data analyses were the same as in Fig. S1*A*. Similar results were obtained in three independent experiments (mean ± SD; $n = 150$ seedlings).

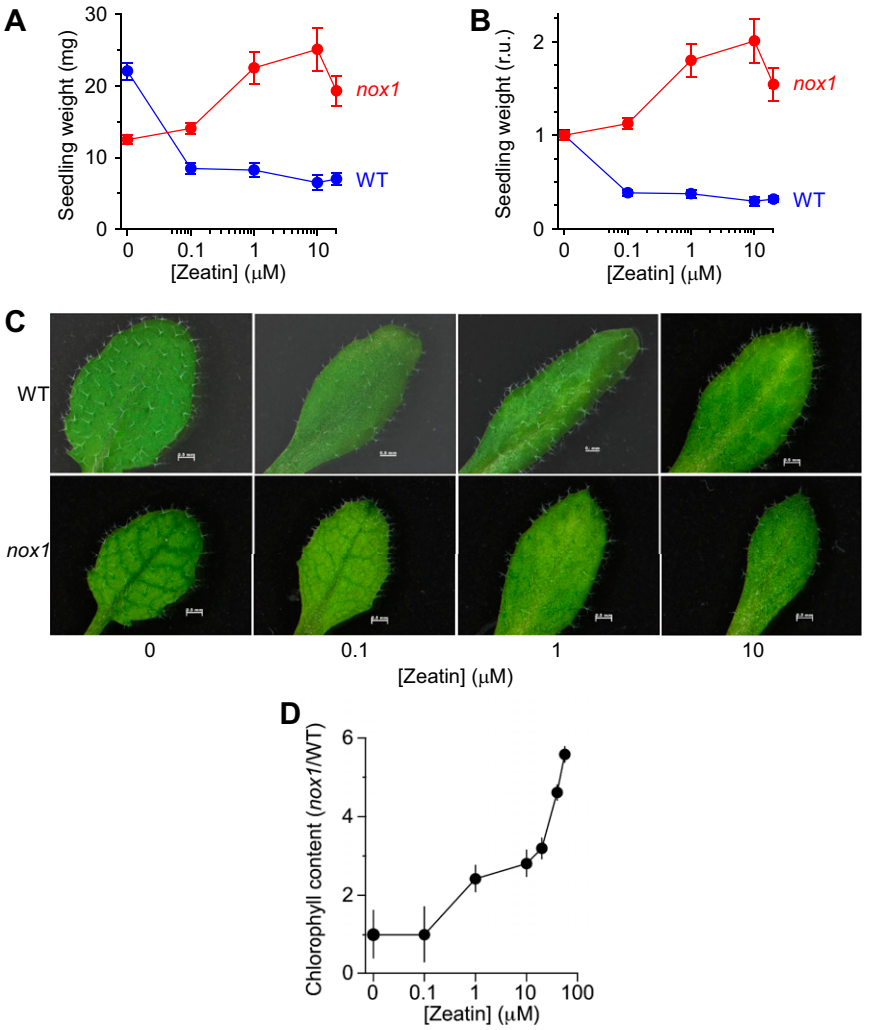

Fig. S3. Zeatin rescues *nox1* phenotype resulting from high levels of endogenous NO. (*A*) The cytokinin zeatin alleviates endogenous NO inhibition of seedling growth in the *nox1* mutant. WT and *nox1* seedlings were grown on MS media containing several concentrations of *trans*-zeatin for 3 wk, and seedling weight was analyzed (mean ± SD; $n = 180$ seedlings). (*B*) Trend analyses of seedling growth in *nox1* and WT in response to *trans*-zeatin from experiments as in *A*. The weight at 0 μM zeatin was arbitrarily set to 1 for both *nox1* and WT (r.u., relative unit). (*C*) Leaf phenotypes of the WT and *nox1* seedlings grown on MS media containing *trans*-zeatin at concentration indicated for 5 wk. (*D*) Quantification of chlorophyll content from the experiments as in *C*. The ratio of *nox1* chlorophyll content and WT chlorophyll content was plotted as a function of applied concentrations of *trans*-zeatin (mean ± SD; $n = 120$ seedlings). The ratio at 0 μM zeatin was arbitrarily set to 1.

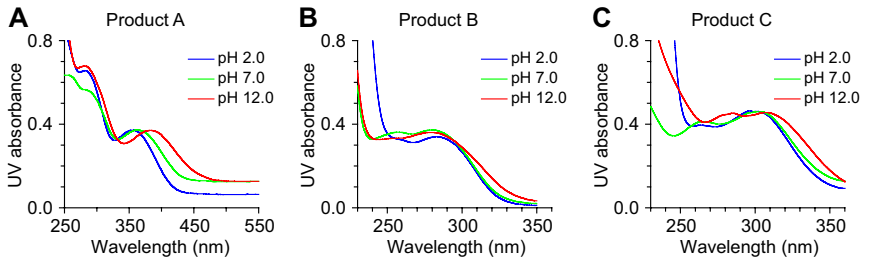

Fig. S4. UV/visible spectra of the three products (A, B, and C) formed in the reaction between zeatin and peroxinitrite as a function of pH. The three products, A, B, and C, were prepared from the reaction of peroxynitrite and *trans*-zeatin in the test tube as described in *SI Materials and Methods*. UV/visible spectra of products A (*A*), B (*B*), and C (*C*) were obtained using buffers with pH 2.0, 7.0, and 12.0, respectively. Experiments were repeated five times and similar spectra were seen.

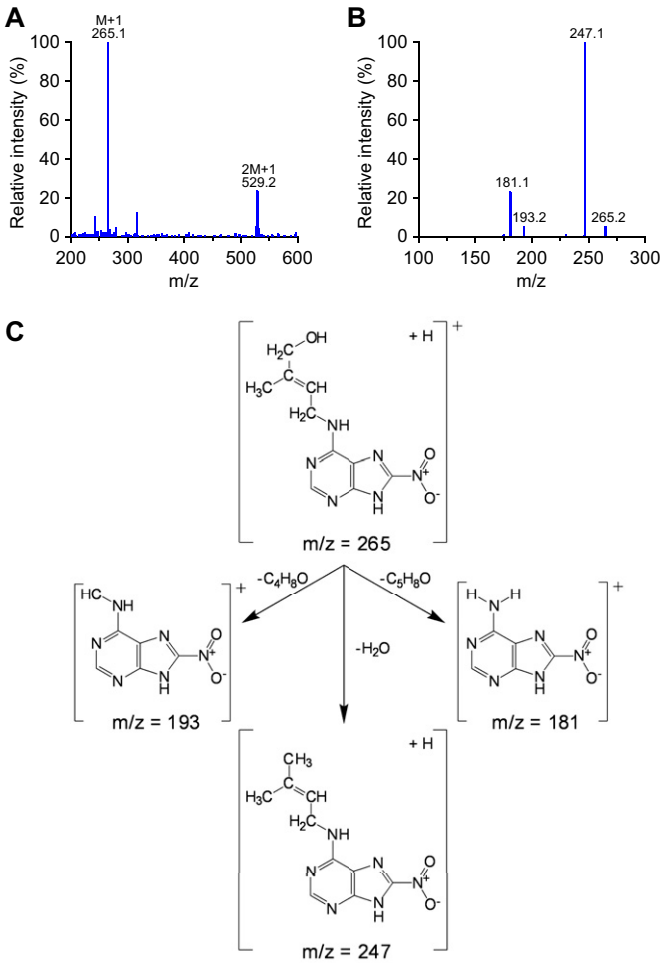

Fig. S5. Characterization of product A using mass spectroscopy. (*A* and *B*) Positive ESI-MS mass spectrum (*A*) and positive ESI-MS/MS mass spectrum (*B*) of product A. Experiments were repeated three times and similar results were seen. (*C*) The major fragmentation reactions and the predicted structures [M + H] based on the LC-MS/MS analyses.

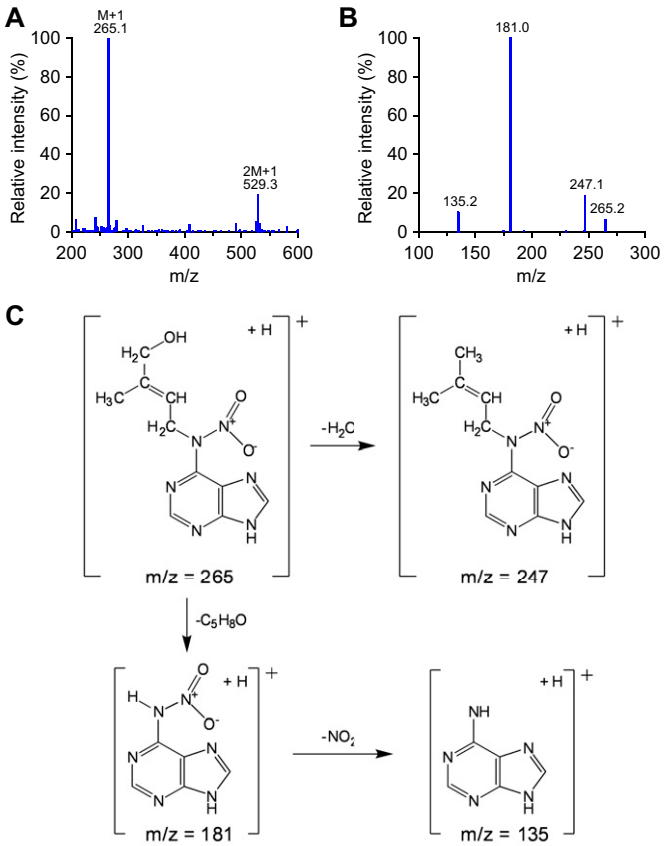

Fig. S6. Characterization of product B using mass spectroscopy. (*A* and *B*) Positive ESI-MS mass spectrum (*A*) and positive ESI-MS/MS mass spectrum (*B*) of product B. Experiments were repeated more than three times and similar results were seen. (*C*) The major fragmentation reactions and the predicted structures [M + H] based on the LC-MS/MS analyses.

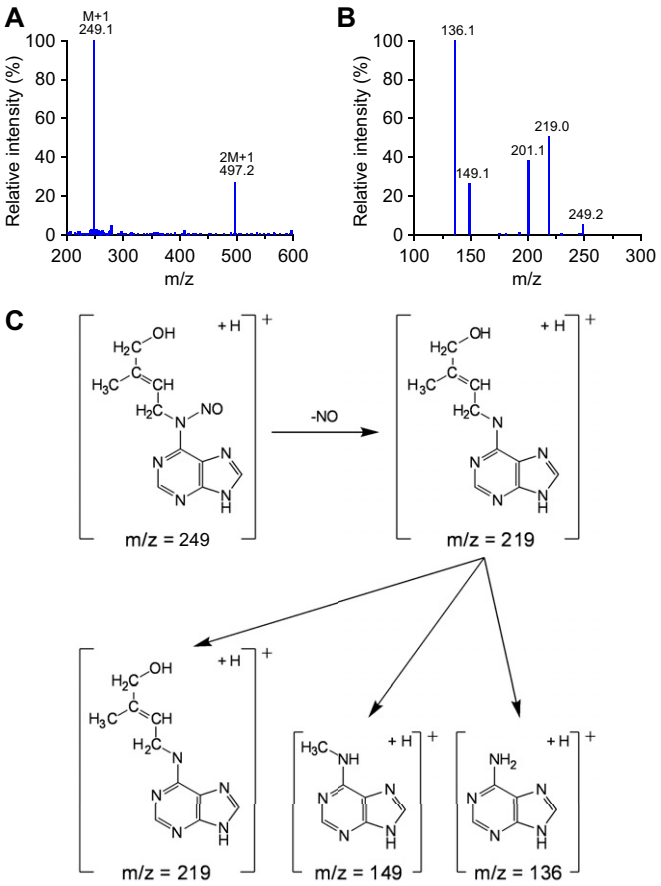

Fig. S7. Characterization of product C using mass spectroscopy. (*A* and *B*) Positive ESI-MS mass spectrum (*A*) and positive ESI-MS/MS mass spectrum (*B*) of product C. Experiments were repeated more than three times and similar results were seen. (*C*) The major fragmentation reactions and the predicted structures [M + H] based on the LC-MS/MS analyses.

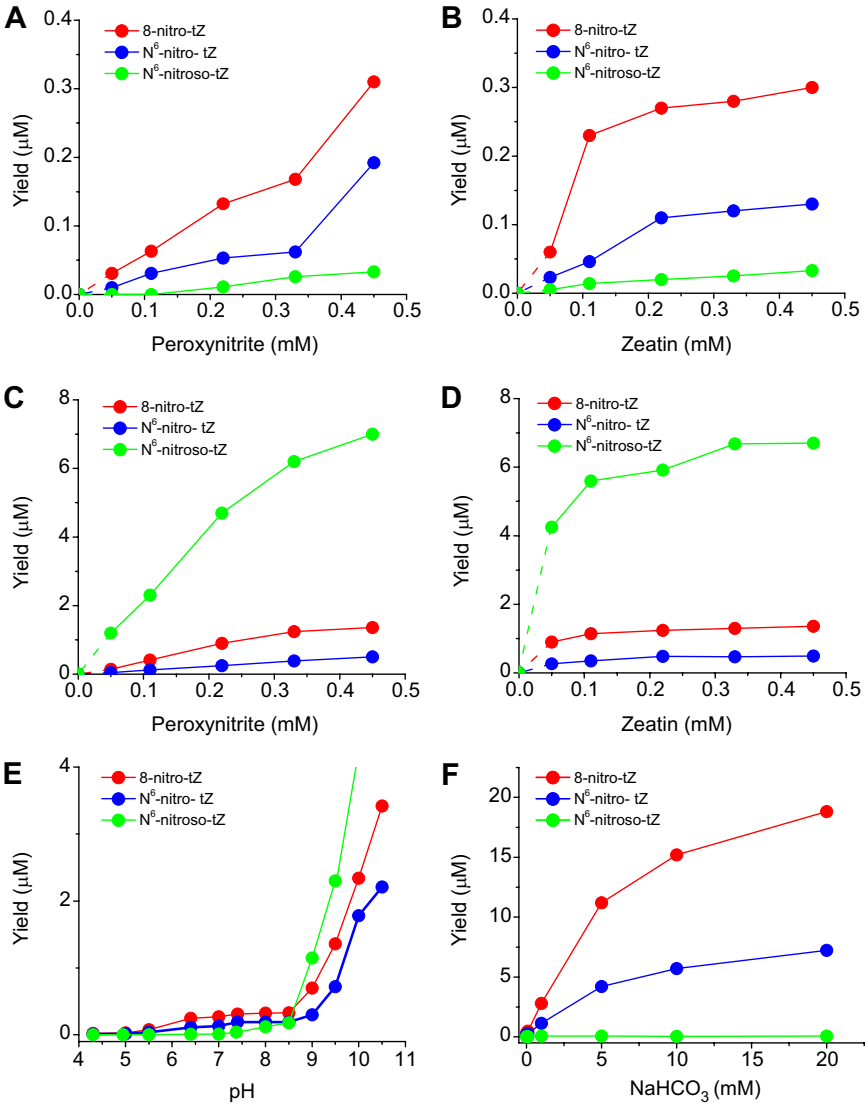

Fig. S8. Exploration of the reaction between *trans*-zeatin and peroxynitrite. (*A*–*D*) Effect of *trans*-zeatin and peroxynitrite concentrations on the yields of 8-nitro-*trans*-zeatin, N^6-nitro-*trans*-zeatin, and N^6-nitroso-zeatin. When studying the effect of peroxynitrite concentration on the yields of three products, the concentration of zeatin was 0.4 mM in sodium phosphate buffer and vice versa. The reactions were carried out at pH 7.4 (*A* and *B*) and pH 9.4 (*C* and *D*). (*E*) Effect of pH on the formation of three reaction products of *trans*-zeatin with peroxynitrite. *Trans*-zeatin (0.2 mM) was incubated with peroxynitrite (0.2 mM) in 100 mM sodium phosphate buffer (pH 4.3–10.5), containing 0.1 mM DTPA at 37 °C for 5 min. (*F*) Effect of CO_2 on the formation of three reaction products of *trans*-zeatin with peroxynitrite. The concentrations of $NaHCO_3$ (0.1–10 mM) enhanced peroxynitrite-mediated nitration of *trans*-zeatin and the yield of 8-nitro-*trans*-zeatin increased remarkably at neutral pH. However, nitrosation was largely not detected under these conditions. This fact indicated that the quotient of 8-nitro-*trans*-zeatin among the three derivatives produced by the reaction between *trans*-zeatin and NO might be depend on CO_2 concentrations. The yields of three products formed in the reaction of $ONOO^-$ with zeatin were determined using purified 8-nitro-*trans*-zeatin, N^6-nitro-*trans*-zeatin, and N^6-nitroso-*trans*-zeatin as standards, respectively. Symbols plot the result of a single representative experiment.

Table S1. NMR spectroscopic data (400 MHz, DMSO-d_6) for products A, B, and C from the reaction of peroxynitrite and *trans*-zeatin

	^{1}H (ppm)				^{13}C (ppm)			
No.	Zeatin	Product A	Product B	Product C	Zeatin	Product A	Product B	Product C
2	8.06	8.13	8.43	8.64	152.4	151.9	154.4	148.3
4	—	—	—	—	149.3	150.0	144.9	147.3
5	—	—	—	—	118.7	122.6	127.2	115
6	—	—	—	—	154.2	156.2	163.7	160.6
8	8.16	—	8.72	8.92	138.6	158.8	148.8	150.9
10	4.11	4.21	4.90	4.92	37.2	37.9	49.6	38.6
11	5.54	5.52	5.61	5.29	120.9	121.0	115.4	114.4
12	—	—	—	—	137.1	138.1	141.6	141.2
13	3.77	3.77	3.74	3.73	65.9	66.2	65.5	65.1
14	1.65	1.65	1.64	1.65	13.7	14.1	13.6	13.7

The three products, A, B, and C, were prepared and purified from the reaction of peroxynitrite and *trans*-zeatin in the test tube as described in *SI Materials and Methods*. ^{1}H and ^{13}C NMR spectroscopic data were recorded on a Bruker DRX 400-MHz instrument in deuterated DMSO-d_6 using standard pulse programs. The characterization of the three purified products was determined on the basis of the comparison of spectroscopy data with zeatin.